MODELING AND SIMULATION OF ELECTRICAL DISCHARGE DEPOSITION OF DIFFERENT MATERIALS

Ana Cristina Iuga[1], Liviu Daniel Ghiculescu[2]
[1] Polytechnic University of Bucharest, Faculty of Industrial Engineering and Robotics, iugaanacristina@gmail.com
[2] Polytechnic University of Bucharest, Faculty of Industrial Engineering and Robotics, daniel.ghiculescu@gmail.com

ABSTRACT: This paper deals with numerical simulation of the deposition of microstructures with two different electrode materials using a dedicated software, COMSOL Multiphysics. An electric discharge deposition process (EDD) can be used to fabricate various metal structures, using a new type of additive technique. The metal is deposited in this process by using the tool electrode's high wear rate as an inverse process of electrical discharge machining. An analysis of the effect of the magnetic field at EDD on two electrodes materials, copper, and tungsten over the substrate was achieved for the purpose of improving the quality of the material deposition. The finite element modeling was parameterized, considering above all the working parameters to determine their influence on the deposition process of the studied materials of electrodes.
KEYWORDS: software, electrical discharge deposition, modeling, simulation, electrode

1. INTRODUCTION

Electrical discharge machining (EDM) has proven extremely beneficial for machining microstructures in hard materials that are difficult to fabricate by conventional means, by melting or vaporization temperatures, which control the material removal [1]. Even though no direct contact exists between the tool and the workpiece, even the most intricate structures and the low resistance materials can be machined without deformation [2]. EDM is regarded as an electrically conductive material removal process with high machining accuracy of several micrometers and surface roughness of Ra 0.05 μm [1]. Therefore, the EDM process has greatly enhanced its capabilities since it emerged more than 80 years ago [3].

Research in recent years shows that tool electrode wear in EDM can be used in the deposition process to create small structures under the right circumstances. This is called the electrical discharge deposition (EDD) technique. The approach undoubtedly introduces a new notion to produce miniature 3D structures [1]. There is an extensive need for hard coatings in industries that require parts to withstand extreme temperatures, stress, chemical corrosion, and other hostile conditions [4]. A thin or thick coating can be produced on the workpiece material using electrical discharge deposition [5].

EDD works on the similar mechanism as EDM, except that the polarity of the electrodes is reversed. The following are the advantages of EDD: with ambient air as a dielectric working environment, the purity of the deposition on the workpiece is determined by the purity of the tool material and its diameter determines the deposition dimension. In general, repetitive discharges between the electrodes cause deposition on the substrate. It is very important for the adhesion of the layers deposition to be controlled by the first layer [6].

In detail, increasing the pulse time from 7,5 μs to 30 μs does not only increase machining time, but also electrode wear rate as well [9]. Moreover, regarding the tribological study conducted, the deposited material has a lower friction coefficient and a specific wear rate [10].
The EDD process of copper and tungsten is reported in this paper. The height and mass of the deposition are increased substantially by magnetic field, while the width is decreased because of plasma restraint.

2. PAREMETERS OF ELECTRICAL DISCHARGES DEPOSITION

The discharge operation involves the application of a voltage between two electrodes (figure 1).

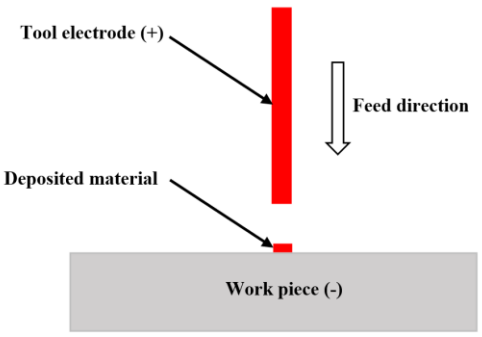

Figure 1. Block diagram EDD process

A mass of electrons is formed when the electrodes are very close together, because of Joule heat and electric field force. When an electric field is applied, the electrons that are emitted are accelerated towards the anode. When electrons collide with particles in a

dielectric medium, they produce a high number of electropositive particles as a result. As a result of this perpetual collision, electrical particles will intensify rapidly throughout the discharge operation, resulting in the formation of plasma channels [7].

As a result of the electrical discharge, the material in the tool electrode melts or gasifies, and the material is removed from the discharge channel before cooling it off over the workpiece surface. A certain amount of material will be removed from the tool electrode and the workpiece during EDD. It is therefore essential that the deposition rate exceeds the removal rate in order to maintain steady deposition. It is therefore very interesting to study EDD deposition in relation to high levels of tool electrode wear.

When the narrow discharge on-time is applied in EDD, the anode's removal amount is much greater than the cathode because of the polarity effect. As a result, this condition facilitates the deposition. Therefore, the tool electrode is the anode in this deposition technology, while the workpiece acts as the cathode, opposite than EDM [1].
Using an EDM machine, the tool advances towards the workpiece by means of servo feed movement on the Z axis (figure 2).

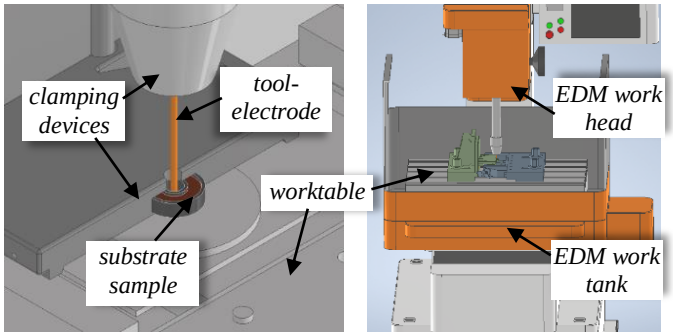

Figure 2. EDM machine used for EDD

The following factors are varied: voltage, current, pulse activation time, and duty factor [8]. Magnetic fields can be used (hybridization of the process) to enhance the quality of the deposited structure, by managing the dimensions of the layers: height, width and consequently the weight.

Several parameters can be changed to perform the deposition process, as shown in table 1. This hybrid process is affected by both EDM parameters (1 – 4) and magnetic flux (5).

Table 1. The parameters of EDD process [8]

No.	Parameters	Values				
1	Voltage (U), [V]	2	30	50	70	98
2	Current (I), [A]	3	9	14	19	25
3	Pulse time (T_{on}), [µs]	7.5	20	30	40	50
4	Duty factor (t)	2	5	7	9	12
5	Magnetic flux, [T]	$5.6\ 10^{-4}$	$1.1\ 10^{-3}$	$1.7\ 10^{-3}$	$5.6\ 10^{-3}$	0.01

3. NUMERICAL SIMULATION OF THE MAGNETIC FIELD AT EDD

In this study, we analyzed the influence of the magnetic field on the EDD process and improved the deposition quality of the conductive tool-electrode materials over the substrate.
For this purpose, the magnetic flux created by the electromagnetic coil and the trajectory of the ion particles were numerically simulated using the following modules of Comsol Multiphysics: 3D - AC/DC - Magnetic Fields - Stationary in stage 1 and Charged Particle Tracing module in stage 2.

Using the parameters from figure 3, the main elements were modeled to simulate the process: anode, coil and working space that stands for the collimator or column. A sample was located at the bottom of the work area - figure 4. The materials of the electrodes used in the deposition process on the sample are copper and tungsten.

Parameters

Name	Expression	Value	Description
Ic	0.4[A]	0.4 A	current in the coil
Nc	3000	3000	number of turns
rbe	8	8	outer radius coil
hb	3	3	coil height
rbi	4	4	inner radius coil
rcol	12.5	12.5	collimator radius
hcol	13	13	column height
scol	3	3	target distance in the column
hc	4	4	cathode height
rc	0.5	0.5	cathode radius
dc	4	4	distant cathode_coil
ECu	7.73[eV]	1.2385E-18 J	initial energy
mCu	63.546*1.66053906660e-27	1.0552E-25	copper ion mass
tpar	0.001*scol/VCu	6.1945E-7	target distance travel time
tp	5e-9	5E-9	study time
Jsz	9000	9000	surface current density
Np	1000	1000	number of particles
VCu	4843	4843	copper ion velocity
tpN	scol/VCu	6.1945E-4	copper ion travel time
tps	10e-4	0.001	copper ion study time
EW	7.98[eV]	1.2785E-18 J	initial energy wolfram
mW	3.05e-25	3.05E-25	wolfram ion mass
tpar	0.001*scol/vW	1.037E-6	target distance travel time
vW	2893	2893	initial speed of ion wolfram
tpN	scol/vW	0.001037	wolfram ion travel time

Figure 3. Parameters of the EDD process

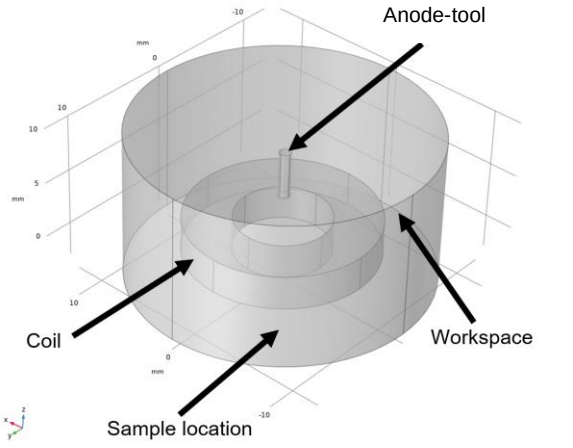

Figure 4. Geometry of the model

The allocation of materials to the model was done as follows: air to the workspace (figure 5), copper (figure 6) and tungsten (figure 7) for the anode as the tool, copper was also used for the coil (figure 6).

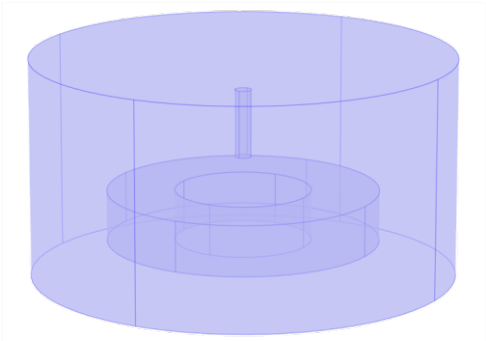

Material Contents

	Property	Variable	Value	Unit
☑	Electrical conductivity	sigma_iso ; sigmaii = sigma_iso, sigmaij = 0	0[S/m]	S/m
☑	Relative permeability	mur_iso ; murii = mur_iso, murij = 0	1	1
☑	Relative permittivity	epsilonr_iso ; epsilonrii = epsilonr_iso, epsilonrij = 0	1	1

Figure 5. Material allocation for the workspace

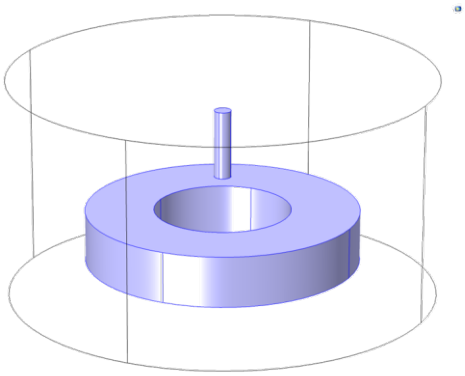

Material Contents

	Property	Variable	Value	Unit
☑	Relative permeability	mur_iso ; murii = mur_iso, murij = 0	1	1
☑	Electrical conductivity	sigma_iso ; sigmaii = sigma_iso, sigmaij = 0	5.998e7[S/m]	S/m
☑	Relative permittivity	epsilonr_iso ; epsilonrii = epsilonr_iso, epsilonrij = 0	1	1

Figure 6. Material allocation for the first tool and coil (Cu)

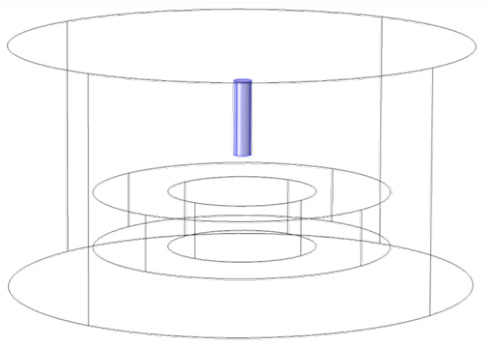

Material Contents

	Property	Variable	Value	Unit
☑	Electrical conductivity	sigma_iso ; sigmaii = sigma_iso, sigmaij = 0	sigma_solid_1(T[1/K])[S/m]	S/m
☑	Relative permeability	mur_iso ; murii = mur_iso, murij = 0	1	1
☑	Relative permittivity	epsilonr_iso ; epsilonrii = epsilonr_iso, epsilonrij = 0	1	1

Figure 7. Material allocation for the second tool (W)

As shown in figure 8, the tetrahedral elements are selected for the mesh, using the finer grade, to ensure the precision of the results. The mesh statistics are presented related to its quality that is evaluated by the ruler placed on the right of the graph.

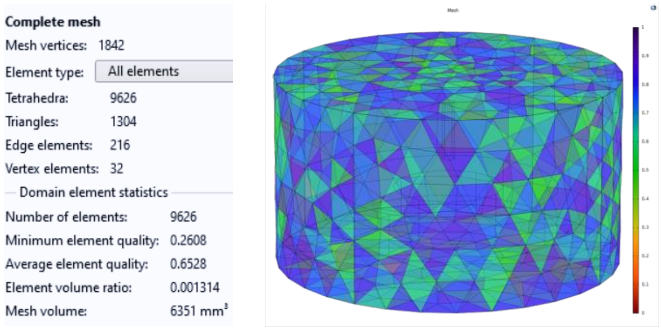

Figure 8. Mesh quality and statistics

The boundary condition for the first module, Magnetic Fields, is the surface current density to determine the magnetic force exerted on the ion beam (figure 9).

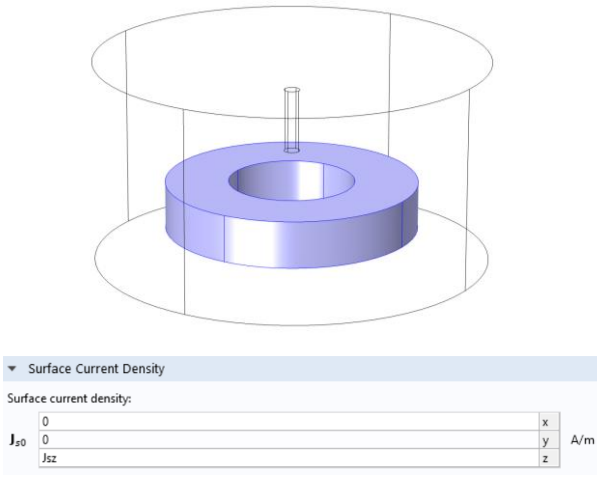

Figure 9. Surface current density on the copper coil

The magnetic field distribution was determined using the first selected module, as illustrated in figure 10.

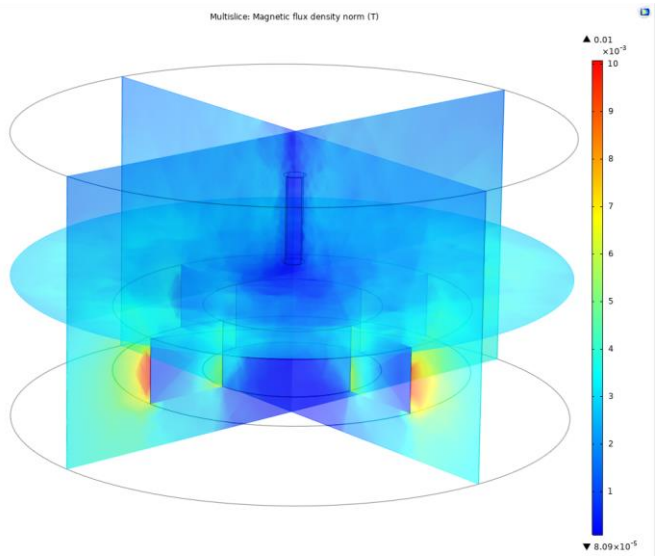

Figure 10. Magnetic flux density

The second study was concerned with determining the trajectory of the ion beam in the work area by tracking the charged particles. Therefore, we considered the magnetic force, which was provided by the magnetic flux density module, used in the first study – figure 11.

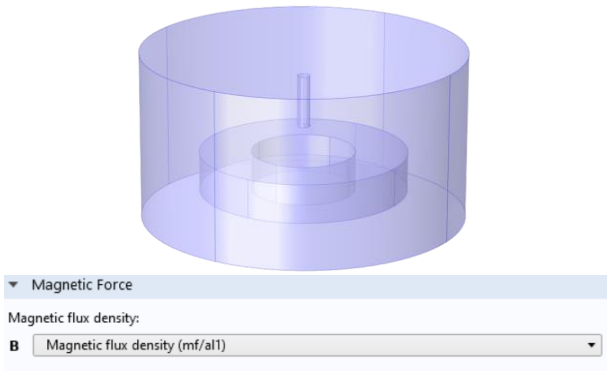

Figure 11. Adding magnetic force to the model

In this case, the study settings are specified by the number of particles released from the highlighted surface and the initial velocity, as well as the entry area of the particles – figure 12.

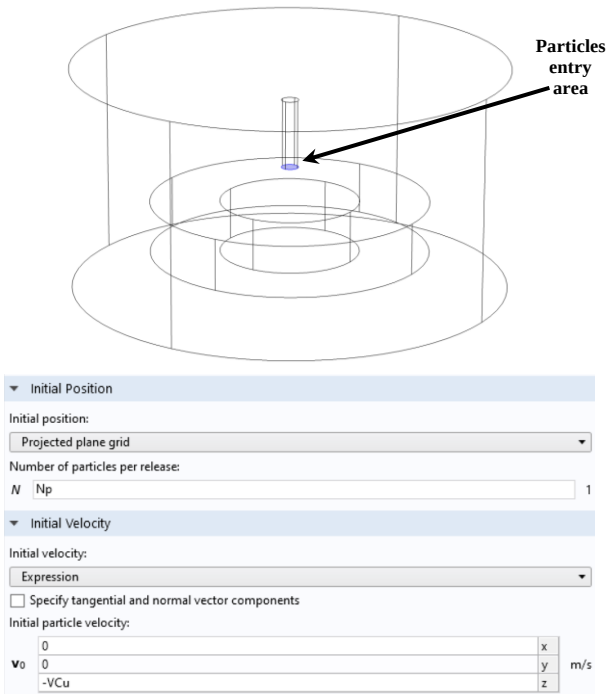

Figure 12. Particle inlet surface and beam inlet settings

To differentiate ion trajectories, particle characteristics were added to distinguish copper and tungsten electrodes – figures 13 and 14.

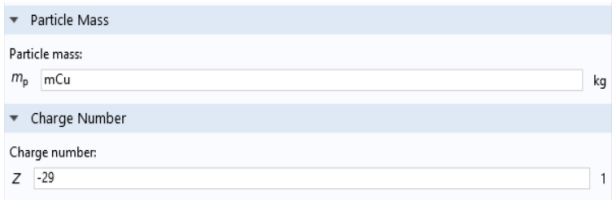

Figure 13. Properties of copper particles

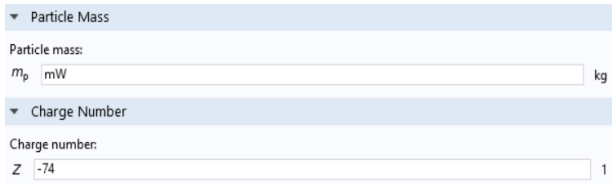

Figure 14. Properties of tungsten particles

As seen in figures 15 and 16, after running the programs, the trajectory of copper and tungsten ions, with higher velocity at copper electrode, is not significantly deflected, thus creating conditions for material deposition on the sample.

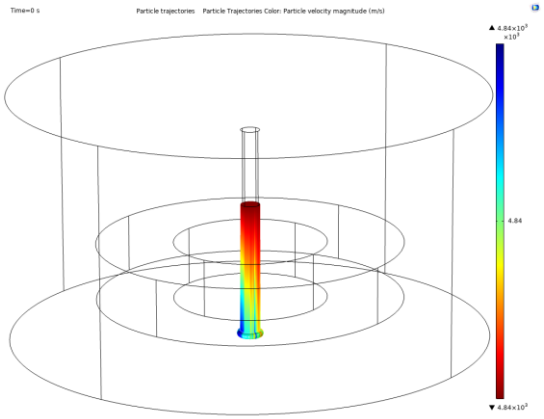

Figure 15. Particle trajectory simulation for copper electrode

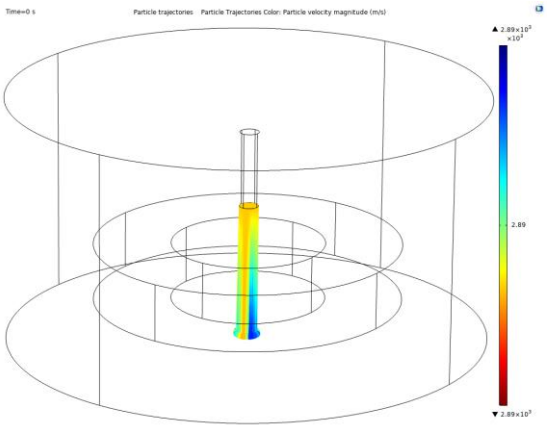

Figure 16. Particle trajectory simulation for tungsten electrode

Using the current surface density (Jsz), Poincaré maps were visualized to determine the deviation of the ion beam trajectory in the working space. Figures 17-19 illustrate the cut planes, depending on Z coordinate, utilized for this purpose.

Figure 17. Cut plane 1 with coordinate Z=4

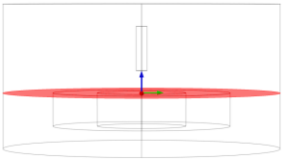

Figure 18. Cut plane 2 with coordinate Z= 2

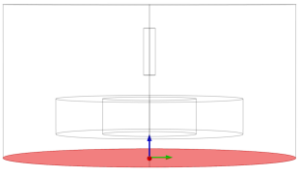

Figure 19. Cut plane 3 with coordinate Z= - 3

4. RESULTS

Aiming at obtaining the same values of the magnetic flux from table 1, the Jsz values were adjusted. The correspondence between these two parameters is presented in table 2, as it resulted from study 1.

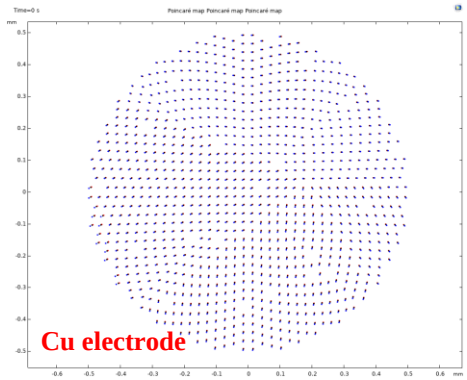

Figure 20. Poincaré map for Jsz = 500 A/mm

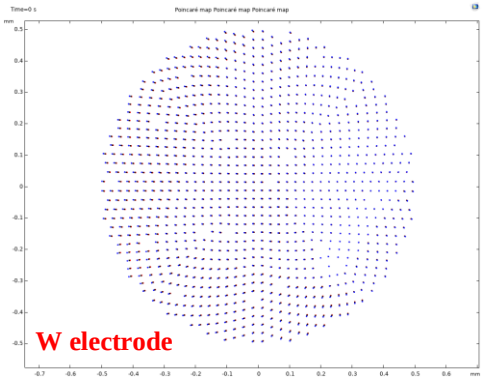

Figure 25. Poincaré map for Jsz = 500 A/mm

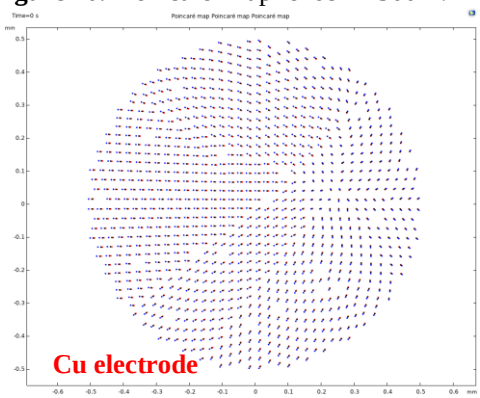

Figure 21. Poincaré map for Jsz = 1000 A/m

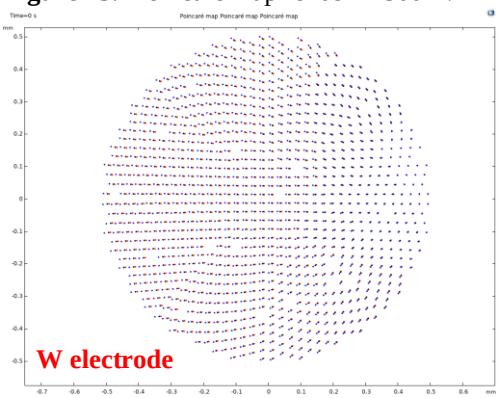

Figure 26. Poincaré map for Jsz = 1000 A/m

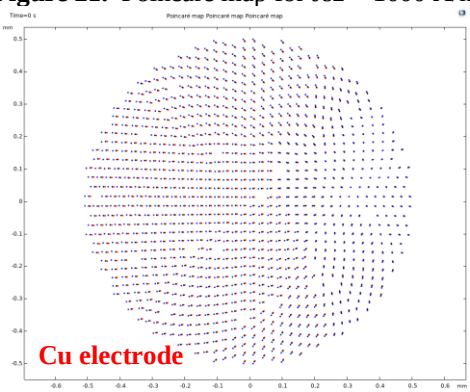

Figure 22. Poincaré map for Jsz = 1500 A/m

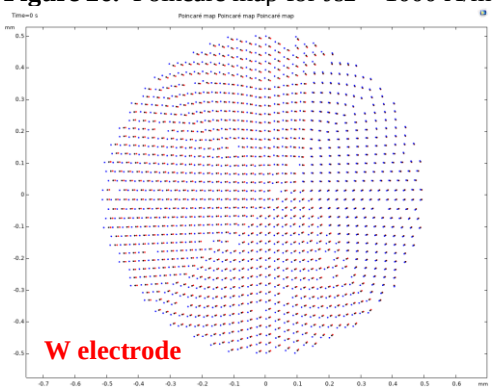

Figure 27. Poincaré map for Jsz = 1500 A/m

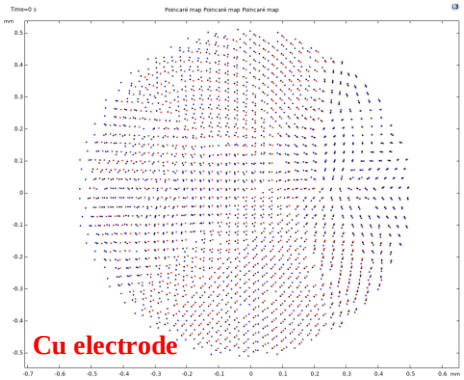

Figure 23. Poincaré map for Jsz = 5000 A/m

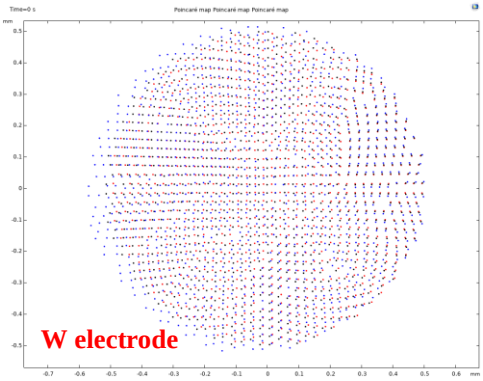

Figure 28. Poincaré map for Jsz = 5000 A/m

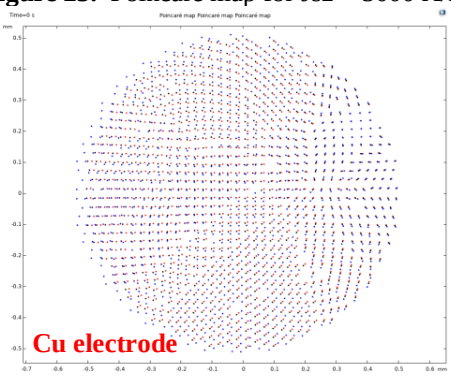

Figure 24. Poincaré map for Jsz = 9000 A/m

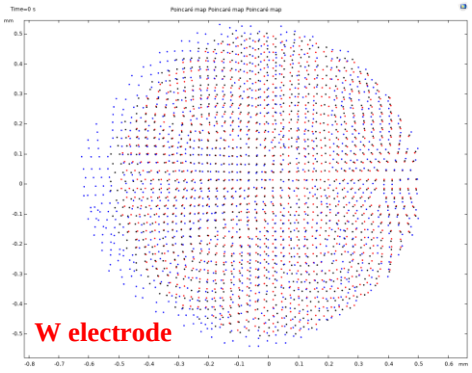

Figure 29. Poincaré map for Jsz = 9000 A/m

Table 2. Surface current density related to magnetic flux

Parameters	Levels				
Magnetic flux, [T]	$5.6 \cdot 10^{-4}$	$1.1 \cdot 10^{-3}$	$1.7 \cdot 10^{-3}$	$5.6 \cdot 10^{-3}$	0.01
Surface current density (Jzs), [A/m]	500	1000	1500	5000	9000

Poincare plots were made comparatively for the two electrode materials: copper (figures 20 – 24) and tungsten (figures 25 – 29). For each previous cut plane, there is a distinct color: Z=4, red; Z=2, black; Z=-3, blue. It can be observed that the deviation of the ion trajectory on the target surface increases as the current density increases.

5. CONCLUSIONS

The study of electrical discharge deposition is based on finite element modeling of the process that comprised two stages: the determination of the magnetic flux inside a column that represents the working space; the determination of the charged particle trajectory, e.g., copper and tungsten ions that are deposited on the sample.

In the process of electrical discharge deposition, the distribution of material on the sample surface is influenced by electrical parameters of the working mode, similar to electrical discharge machining, namely voltage, current, pulse, and pause times, and essentially the polarity, able to produce high wear of the tool-electrode. The current within the electromagnetic coil as well as its dimensions also play a significant role.

An increase in surface current density led to a larger and more irregular distribution on the sample that resulted, comparatively with an appropriate distribution when a mean magnetic flux was used. The Poincare plots show that the trajectory of the ions is more dispersed in case of tungsten due to the higher atomic number, Z=74.

Moreover, the atomic mass of copper, and consequently a higher particle speed than tungsten, like 4843 m/s, helps the trajectory to be linear, this being dispersed more at higher Jsz value, e.g., 5000 A/m.

Further experiments are required in order to validate the numerical simulation and to gain a deeper understanding of electrical discharge deposition mechanism aiming at precision and surface quality improvement.

6. REFERENCES

1. Zilong P, Guan X, Micro Electrical Discharge Machining Deposition in Air for Fabrication of Micro Spiral Structures, *Chinese Journal of Mechanical Engineering*, Vol. 23, No. 2, pp. 154-160, (2010).
2. Kansal H.K. et.al, Technology and research developments in powder mixed electric discharge machining (PMEDM), *Journal of Materials Processing Technology*, Vol. 184, No.1-3, pp.32-41, (2007).
3. Y.F. Luo, The dependence of interspace discharge transitivity upon the gap debris in precision electro-discharge machining, *J. Mater. Process. Technol.*, Vol. 68, pp.127–131, (1997).
4. Liew P. et.al., Surface modification and functionalization by electrical discharge coating: a comprehensive review, International *Journal of Extreme Manufacturing*, Vol. 2, No. 1, 32 pp, (2020).
5. Elaiyarasan U., et.al., Response surface methodology study on electrical discharge deposition of AZ31B magnesium alloy with powder composite electrode, *International Journal on Interactive Design and Manufacturing (IJIDeM)*, (2022).
6. Jitendra K, Janakarajan R, Dhamodaran S, Kanmani S., Dry Micro-Electric Discharge Deposition of Copper on Die steel: Effect of Pulse on-time, *International Workshop on Micro Factories*, Vol. 7, No.1-4, (2010).
7. ZhenLong W, JingZhi C, BaiDong J, Study on Micro Electrical Discharge Deposition in Air, *International Conference on Mechatronics and Automation, IEEE*, pp. 63-68, (2007).
8. Murlidharan B, Chelladurai H, Janakarajan R, Experimental Investigation on Electro-Discharge Deposition Process, *The International Journal of Advanced Manufacturing Technology*, Vol, 76, pp. 69–82, (2015).
9. Tsui H., Hsu S., Study on Fe-Based Metallic Glass Micro Hole Machining by Using Micro-EDM Combined with Electrophoretic Deposition Polishing, *Processes*, Vol. 10(1), 96, (2022).
10. Rajeshshyam R. et.al., Process Optimisation and Tribological Behaviour Studies on Surface Modified Al 6061-T6 Alloy Deposited with WS2 Solid Lubricant Layer Through Electrical Discharge Approach, *Arabian Journal for Science and Engineering*, 47, pp. 8009–8030, (2022).